Canadian Journal of Pure and Applied Sciences
Vol. 15, No. 2, pp. 5231-5238, June 2021
Online ISSN: 1920-3853; Print ISSN: 1715-9997
Available online at www.cjpas.net

WEIGHT, MASS, ENERGY, TEMPERATURE, PERMITTIVITY, PERMEABILITY, AND CHEMISTRY DETERMINE REFRACTIVE INDICES

Stephen Arthur Langford
Langford Consulting, Danielson, Connecticut, USA

ABSTRACT

In the previous paper, assumption of a Vacuum Structure led to creation of predicted and residual models for rest mass (*m*), energy (*E*), and weight (*W*). Those models were based **only** upon prior work by Galileo, Newton, Einstein, Planck, and de Broglie; experimentally estimated refractive-index (RI) probability levels and related temperature data **not** having been considered. Here, the question of how best to model the statistic ***(L%+E%)***, against those factors of Quantum Mechanics (QM), is explored. (***L%***) is the statistical cumulative-frequency-distribution surface and (***E%***) is the statistical-density-function surface. Variables based upon temperatures set for immersion liquids and those estimated also for immersed-fragment interiors are found nicely to improve the QM-only models. These results demonstrate at least one realm in which QM aspects interrelate seamlessly with the so-called "Real World" of statistically-significant RI data sets generated by a mere experimental human.

Keywords: Vacuum Structure, refractive indices, Optical Mineralogy, de Broglie, rest mass, energy, weight, permittivity, permeability.

INTRODUCTION

In (Langford, 2021b) – for the visible-light portion of the Electromagnetic (EM) and the 1.40-1.80 (inclusive; unitless) refractive-index (RI) range of minerals in the subject gabbroic rock powder – predicted and residuals models for rest mass (*m*), energy (*E*), and weight (*W*) were developed, graphically presented, and briefly discussed. Here, a series of three (3) regressions, styled to emulate general linear modeling (GLM), were performed and analyzed, employing the SAS JMP Pro v.15.2.1 statistical package (Courtesy SAS).

Some fundamentals mentioned on the first page of the paper by Langford (2021b) will be also used here below. However, it is necessary to mention here anew that the Refractive indices (RIs) are often denoted by "n" and Refractivity is defined to be "RI-1". An italicized vee (*v*, standing for "velocity") looks like the Greek letter nu (*ν*, not to be seen again in this paper below). So, RI = $n = c/v$, $nv = c$, and $v = c/n$. Also, the wavelength $\lambda = h/mv$ is written by de Broglie. The symbol for mass (*m*) is herein colored red, in contradistinction to meters (m). Planck's constant (h) is defined exactly to be $6.62607015 \times 10^{-34}$ [J×s] (Newell and Tiesinga, 2019). The wavelengths (λ, nm) convert to meters (m); for example, 589.3 [nm] = 5.893×10^{-7} [m]. The speed of light *in vacuo* is $c = 299{,}792{,}458$ [m/s]. De Broglie's $\lambda = h/mv$ converts to $mv\lambda = h$, leading by substitution to $m = h/v\lambda = h/(c/n)\lambda$. Also, the liquid refractive indices (RIs; unitless) were rounded to only 6 significant places beyond the decimal point. So, let's introduce the problems and the modelling described in the following sections.

Corresponding author e-mail: gambist@gmail.com

Problems encountered when using GLM

After sadly and with alarm discovering that computer runs in GLM of the same data, with the same GLM settings, were producing different statistical-regression results; and, that what had been thought to be running GLM in JMP was not exactly doing so (personal communication, Bradley Jones, Principal Research Fellow at the JMP division of SAS): Subsequently, Sue Walsh (JMP Technical Support) kindly showed the author how to configured JMP analyses to duplicate a GLM output from Statistica (created by StatSoft and lately a TIBCO Software product), for the same data set. Here is a Précis of Ms. Walsh's instructions:

Summary of Sue Walsh's GLM Recipe (with a few additions), for Users of the JMP Fit-Model Module

- 01. Ensure by seeing a blue triangle next to each variable that JPM has it as numeric and continuous.
- 02. Select Analyze | Fit Model.
- 03. In the Model Specification Window, select the response (dependent) variable; click on Y.
- 04. Select all independent variables and click on Add (or click and drag, in the order desired).

- 05. Change alpha level to 0.01, by clicking on red triangle next to Model Specification and selecting Set Alpha Level.
- 06. Type in 0.01, then click OK.
- 07. Ensure that Personality is set to Standard Least Squares and Emphasis is Effect Leverage.
- 08. Click radio button Keep Dialog Open.
- 09. Choose No Intercept, when appropriate.
- 10. Choose Degree 3 or more, if default 2 setting is not desired.
- 11. Click on Run.

MODELING VIA THREE (3) REGRESSIONS

Table 1. The list of independent variables and constants entered into at least one of the three regressions run to fit dependent variable ***(L%+E%)*** in the JMP. The reader can see them in the context and Figures 1, 2, 3, 4, and 5.

Independent Variables	**Meaning**
m(kg)e38	Estimated mass in kilograms, raised to the 38^{th} power
m(kg)rs	Residual mass (*m*) in kilograms
(E•J)^20	Energy in Joules, raised to the 20^{th} power
(E•J)^20rs	Residual energy (*E*) in Joules, raised to the 20^{th} power
W•N•E36	Weight in Newtons (N), raised to the 36^{th} power
W•N•E36rs	Residual weight in Newtons (N), raised to the 36^{th} power
c•(m/s)	Speed of light in *vacuo* (*c*), in meters (m) per second (s)
c^2(m^2/s^2)	$[\mathbf{c•(m/s)}]^2$
c^3(m^3/s^3)	$[\mathbf{c•(m/s)}]^3$
g•m•s	Author's estimations of *g*, based upon two (2) different laboratory elevations; m/s.
h(J·s)	Planck's constant h = 6.62607015 × 10^{-34} [J×s]
StgLqT°C	Immersion-liquid temperature *T* [°C]; assumed to be set stage *T* [°C]
StgLqT°C^2	The variable **StgLqT°C** squared
StgLqT°C^3	The variable **StgLqT°C** cubed
PrtclT°C	Backwards estimate of temperatures inside immersed powder fragments
PrtclT°C^2	The variable **PrtclT°C** squared
PrtclT°C^3	The variable **PrtclT°C** cubed
HotrBy°C	**HotrBy°C = PrtclT°C – StgLqT°C**

Table 1 lists the variable names used in at least one (1) of the three (3) regressions. However, 1) to generate the greatest possible number of significant digits in resulting coefficients and 2) to provide each variable or constant with equal footing in the regressions: All data were scaled to fall within the zero (0) to unity (1) range. In order to preserve what was left of sanity, no changes were made to the variable names when that scaling was done.

The first of the three regressions included all of the "variables" [purposefully, "stupidly" including constants] on the right side of the equation suggested by "throwing the kitchen sink" at dependent variable ***(L%+E%)***:

(*L%+E%*)=f[(m(kg)e38, m(kg)rs, (E•J)^20, (E•J)^20rs, W•N•E36, W•N•E36rs, c•(m/s), c^2(m^2/s^2), c^3(m^3/s^3), g•m•s, h (J·s), StgLqT°C, PrtclT°C, HotrBy°C]

JMP Pro v.15.2.1 produces a plethora of output for each regression, the setup for each of which is available in the aforementioned work logs posted online. Only those portions pertinent to this analyst's thinking are reproduced here, as in Figure 1, from the first-regression report.

Singularities noted for the Intercept and **m(kg)e38** ($m \times 10^{38}$ [kg]) were not seen to demand immediate abandonment of either that variable or of the choice to use an Intercept in the modeling. The 2D image of the 3D data is not helpful. But the first three variables listed in the LogWorth Effect Summary have to do with Galileo's work on gravity and Newton's $f = ma$, cast here as $W = mg$ (whatever mass may be). It is notable that the value of g (gravity estimated at each of two labs) – estimated merely by very rough guesses as to elevations with respect to each of the two laboratories where data were gathered – features in both variable **g•m•s** and **W•N•E36rs**. During later model refinement (but not in this paper), those g estimates will be improved upon, via backwards estimation.

Recast Second Regression Model

An error in independent-variable filtering led later to re-doing this model. After a bit of scrambling, the setup was configured as shown in Figure 2, wherein note that the intercept was dropped and Degree was changed to 3, replacing the default 2 setting. Figure 3 shows the pertinent results reported by the second GLM-emulating JMP regression.

Variable **W•N•E36rs** was next retained, in order to discover how it would fare in the model to include higher powers of liquid and particle temperatures. Figures 4 and 5 show, respectively, 1) the setup for the final model presented here and 2) the important portions of JMP Pro statistical output for that model.

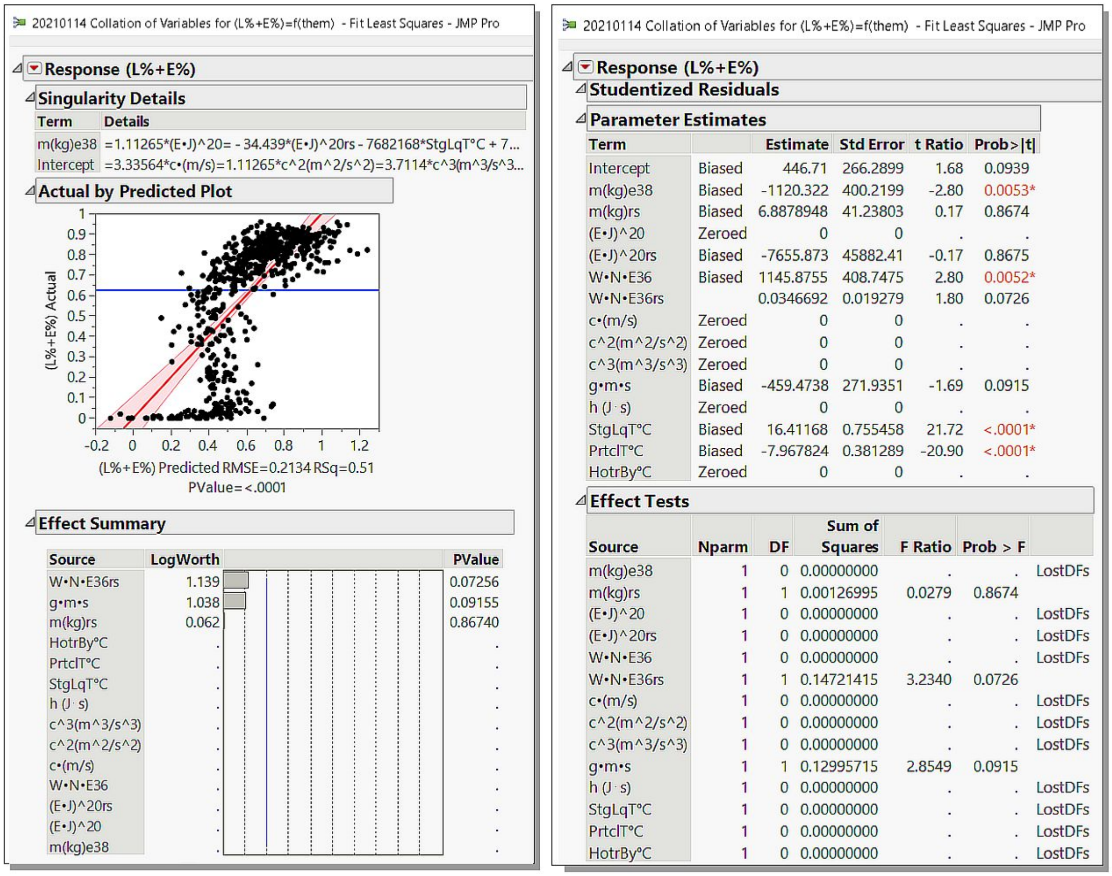

Fig. 1. The results from JMP Pro v.15.2.1 Fit Model; after the first of three regressions.

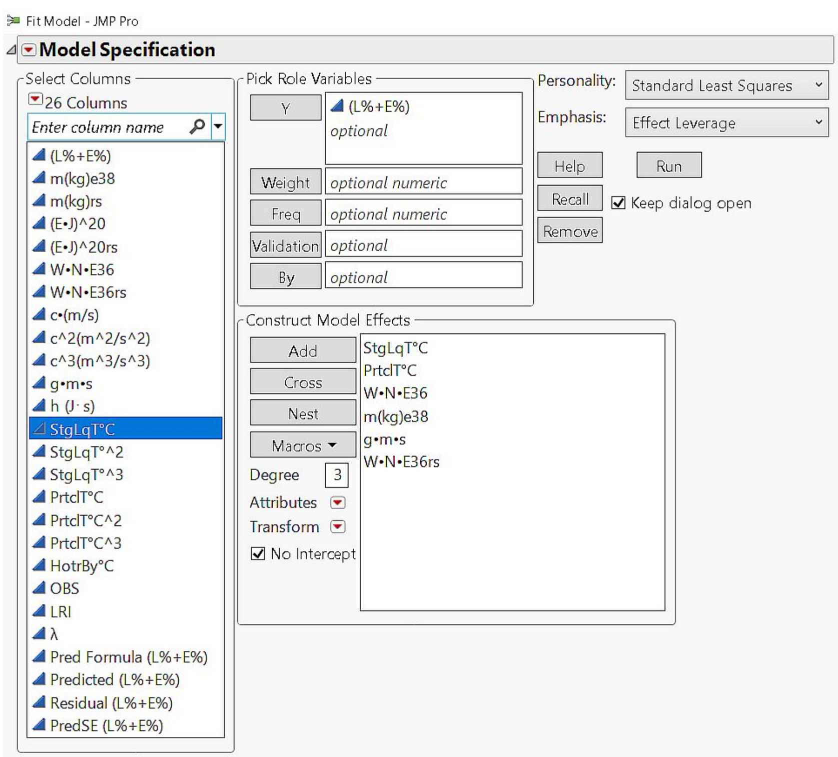

Fig. 2. The third setup for the second modeling run.

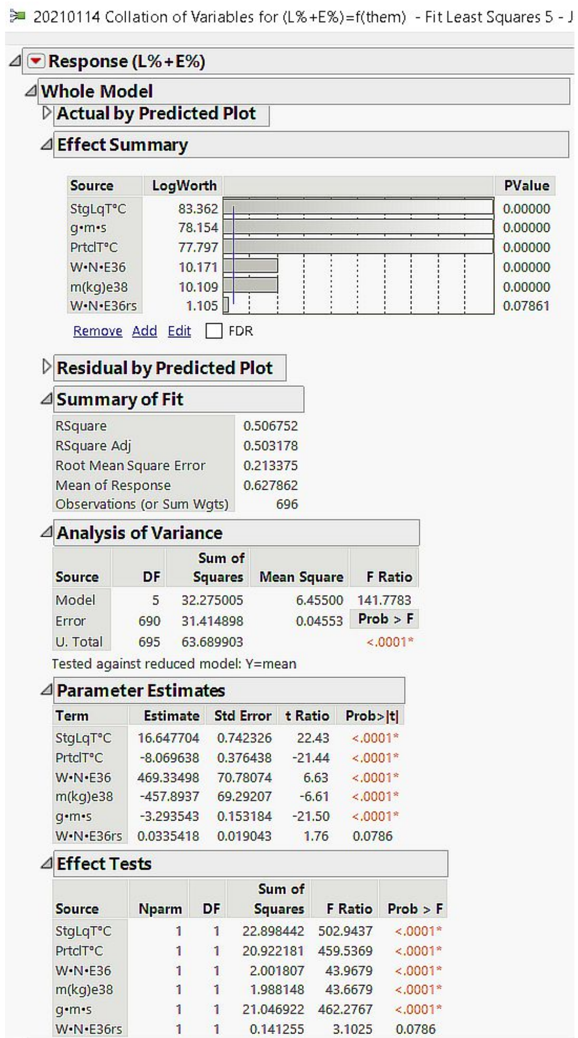

Fig. 3. The partial JMP Pro v.15.2.1 output for run set up as in Figure 2.

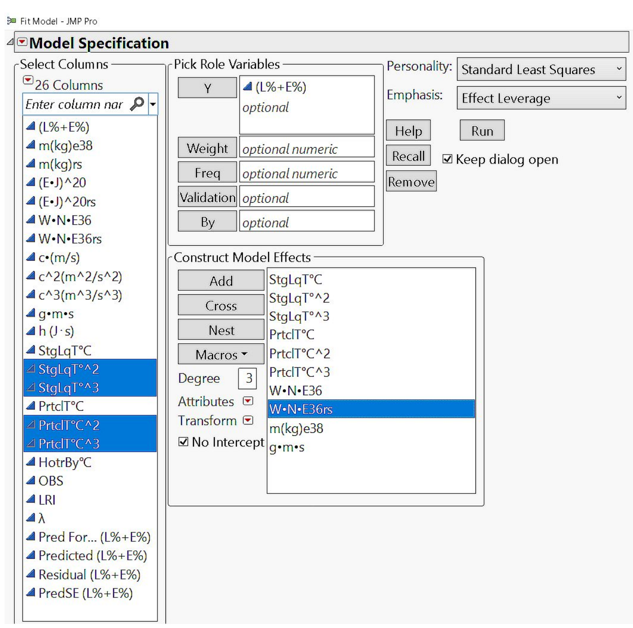

Fig. 4. The setup for the final model of this work.

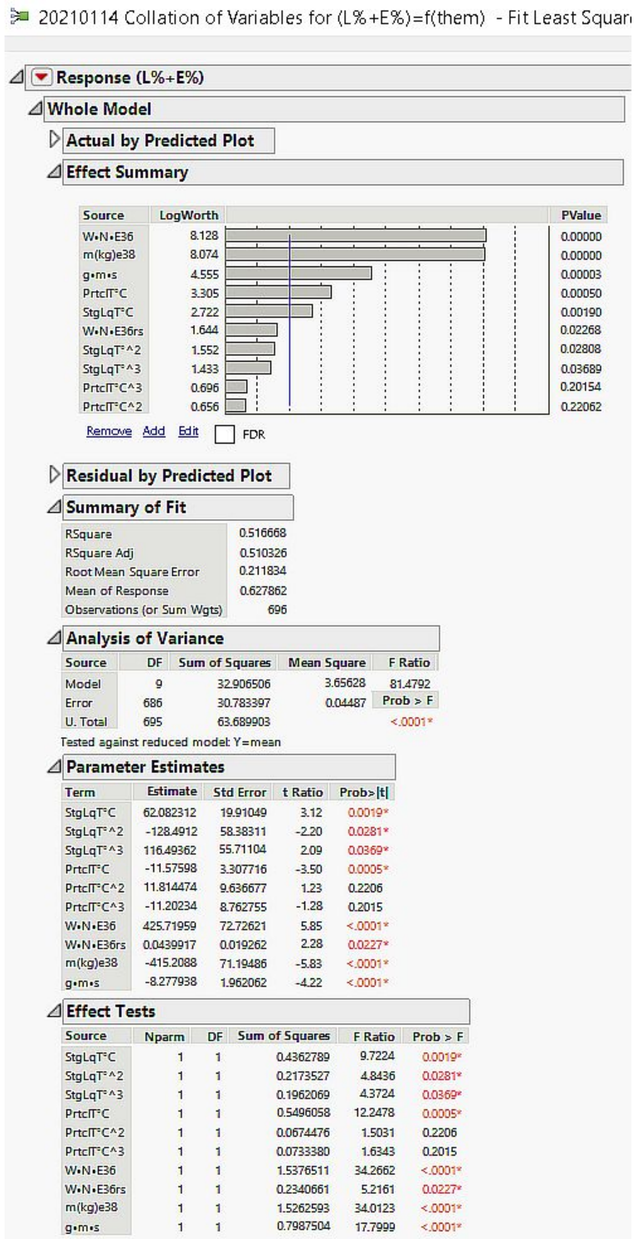

20210114 Collation of Variables for (L%+E%)=f(them) - Fit Least Squar

Response (L%+E%)

Whole Model

Actual by Predicted Plot

Effect Summary

Source	LogWorth	PValue
W•N•E36	8.128	0.00000
m(kg)e38	8.074	0.00000
g•m•s	4.555	0.00003
PrtclT°C	3.305	0.00050
StgLqT°C	2.722	0.00190
W•N•E36rs	1.644	0.02268
StgLqT°^2	1.552	0.02808
StgLqT°^3	1.433	0.03689
PrtclT°C^3	0.696	0.20154
PrtclT°C^2	0.656	0.22062

Remove Add Edit FDR

Residual by Predicted Plot

Summary of Fit

RSquare	0.516668
RSquare Adj	0.510326
Root Mean Square Error	0.211834
Mean of Response	0.627862
Observations (or Sum Wgts)	696

Analysis of Variance

Source	DF	Sum of Squares	Mean Square	F Ratio
Model	9	32.906506	3.65628	81.4792
Error	686	30.783397	0.04487	Prob > F
U. Total	695	63.689903		<.0001*

Tested against reduced model: Y=mean

Parameter Estimates

Term	Estimate	Std Error	t Ratio	Prob>|t|
StgLqT°C	62.082312	19.91049	3.12	0.0019*
StgLqT°^2	-128.4912	58.38311	-2.20	0.0281*
StgLqT°^3	116.49362	55.71104	2.09	0.0369*
PrtclT°C	-11.57598	3.307716	-3.50	0.0005*
PrtclT°C^2	11.814474	9.636677	1.23	0.2206
PrtclT°C^3	-11.20234	8.762755	-1.28	0.2015
W•N•E36	425.71959	72.72621	5.85	<.0001*
W•N•E36rs	0.0439917	0.019262	2.28	0.0227*
m(kg)e38	-415.2088	71.19486	-5.83	<.0001*
g•m•s	-8.277938	1.962062	-4.22	<.0001*

Effect Tests

Source	Nparm	DF	Sum of Squares	F Ratio	Prob > F
StgLqT°C	1	1	0.4362789	9.7224	0.0019*
StgLqT°^2	1	1	0.2173527	4.8436	0.0281*
StgLqT°^3	1	1	0.1962069	4.3724	0.0369*
PrtclT°C	1	1	0.5496058	12.2478	0.0005*
PrtclT°C^2	1	1	0.0674476	1.5031	0.2206
PrtclT°C^3	1	1	0.0733380	1.6343	0.2015
W•N•E36	1	1	1.5376511	34.2662	<.0001*
W•N•E36rs	1	1	0.2340661	5.2161	0.0227*
m(kg)e38	1	1	1.5262593	34.0123	<.0001*
g•m•s	1	1	0.7987504	17.7999	<.0001*

Fig. 5. The statistical report for the final model of this work.

THE FINAL MODEL

A plethora of details related to JMP Pro v.15.2.1 modeling and to Surfer® modeling, including numerous statistical reports, is posted in Work Logs to be found at https://tinyurl.com/yn8brkd7. Perspective and plan-view images for the final Predicted, |Residuals| and Total={Predicted+|Residuals|} Models are shown in Figure 6. However, an extremely-high-resolution version of Figure 6 is available at https://tinyurl.com/2cge2el7 (it may require considerable time to download), where one can clearly read the digits of the surface equations and appreciate other, finer details not easily seen in the figure shown here.

Figure 7 shows a lower, "arrow head" growth of probable Pigeonite (Augitic Clinopyroxene), emerging from a sea of what seems to be a "nurturing wrap" of Olivine; together with a closer (just to the left), higher growth of probable Olivine. Please note that the image is of probability levels, not actually of what the author calls (for want of a possibly more-appropriate term) "growths" or "crystallites". The shapes are interpreted to be displaying different incipient crystal habits, which do not seem to presage those most-commonly to be found in hand specimens of those minerals; the "incipient habits" are simply interpretations that might be incorrect.

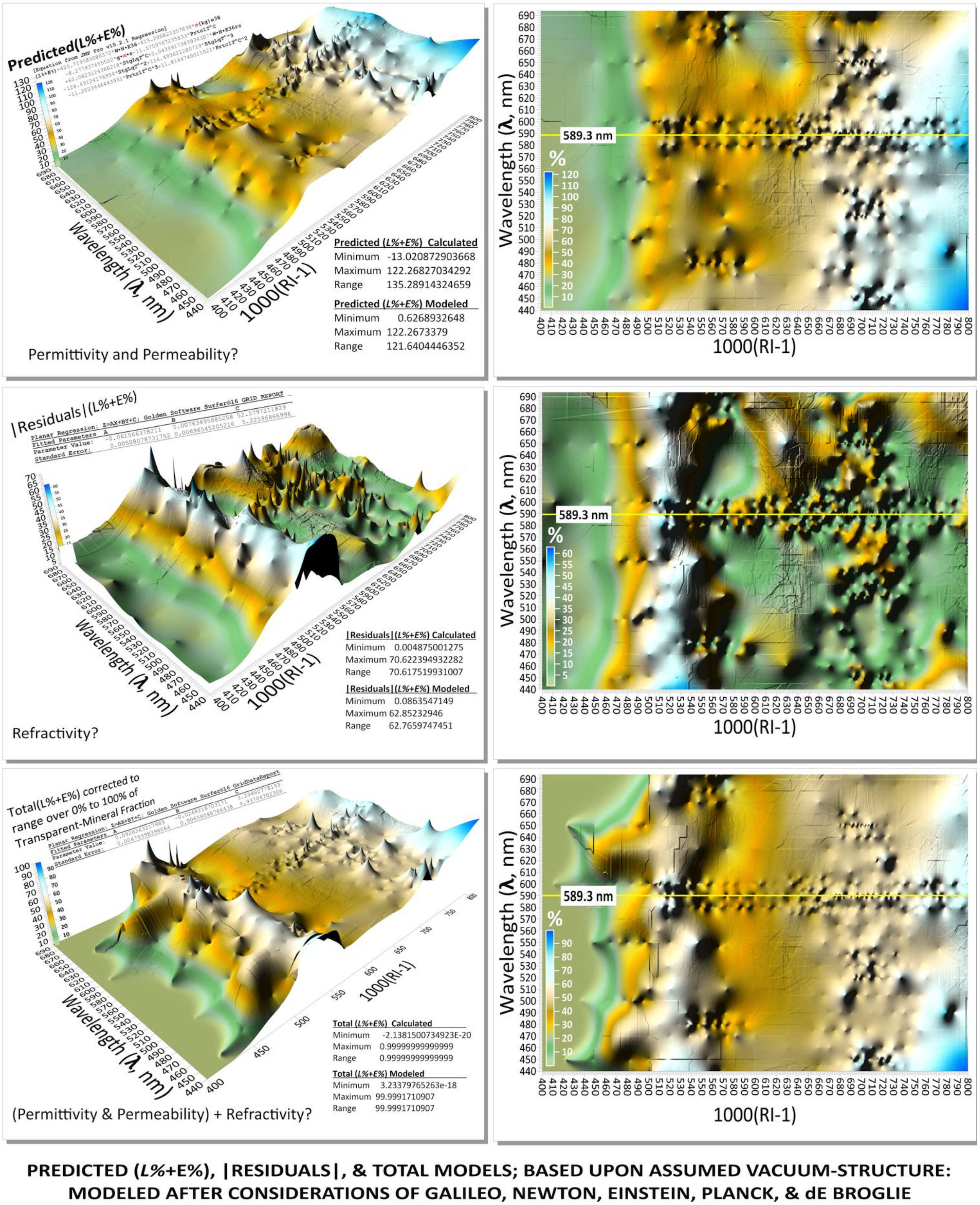

Fig. 6. The perspective and plan-view images for the final Predicted, |Residuals|, and Total = {Predicted + |Residuals|} Models.

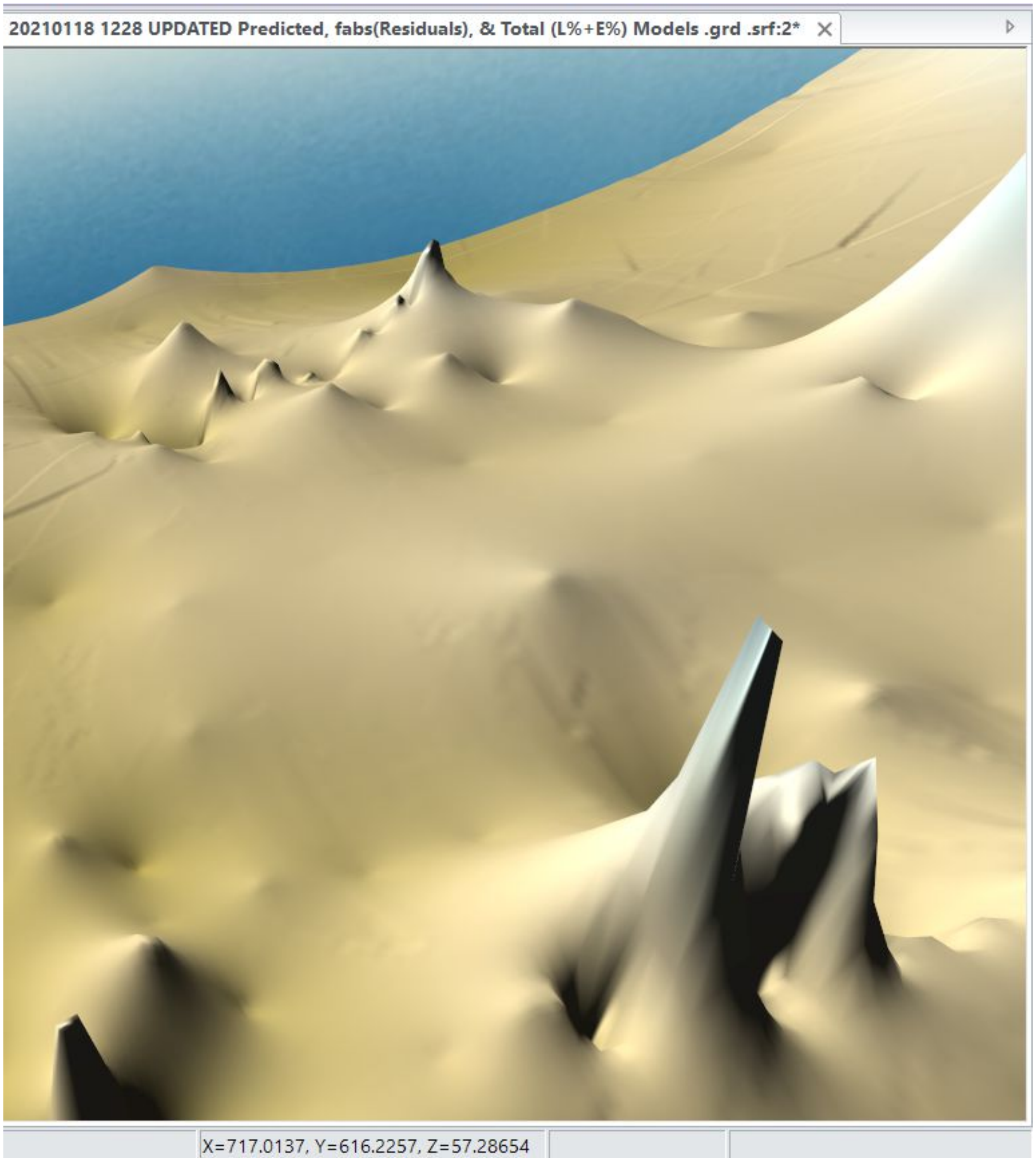

Fig. 7. The possible Olivine and Pigeonite "crystallites", emerging from a field of Olivine.

DISCUSSION

As anticipated, variable **W•N•E36rs** fared well in the LogWorth reported in Figure 5. It is surprising how well **g•m•s** fared, since the elevation estimates upon which it is based were so casually made. The higher orders of liquid and particle temperatures spread the important temperature effects across a total of six independent variables. Mass (*m*), gravity (*g*), weight (*W*), and Temperatures (*T*, °C) estimated – both for liquids and for fragment interiors – are the major factors found to be determining ***(L%+E%)*** probability levels. $E = mc^2$ fell out of consideration not because it is unimportant but because 1) *m* is separately and nicely modeled in variable **m(kg)E38**, and 2) values of *c* (related definitionally to RI) are contained within RI variable ***(L%+E%)***, making it an "illegal" "independent" (which it isn't) variable.

In (Langford, 2021b), topologies are mapped without reference to RI data. They therefore seem to be mapping permittivities and permeabilities that resemble topologies previously obtained (Langford, 2021a) from RI data. Here, Figure 6 raises the questions: Are permittivities and permeabilities being mapped separately from refractivities in the respective Predicted and Residuals Models? Or are permittivity and permeability effects being mixed with RI effects throughout, as seems to be more probable?

Although "Chemistries" is in the title of this paper, the only chemical analysis done to date on subject sample FUD27 is the bulk-chemical analysis available at https://tinyurl.com/3bvf66ob. Perhaps a day will come when others – possessing sophisticated, modern equipment – will sort minerals for this or a similar sample from the same Ukumehame Gulch, West Maui, Hawai'i stock, sorting out fragments displaying RIs near 1.7170RI and 616.2 nm (coordinates in Figure 7), and then performing modern chemical analyses (to include trace elements) on them. Dispersion-staining methods (McCrone *et al*., 1968) might be useful in such work, though liquid-immersion work on very fine powders is more likely to produce results with higher precisions than are available from thin-section work.

A tantalizing chicken-or-the-egg question seems to be whether mineral chemistries might actually be determined by positions on the Emmons Surface: Are only certain chemistries permitted at each such point? If not, what ranges of chemistries might one find at essentially single points on the Emmons Surface? Future work soon to be written will focus upon how results from this work might, through backwards-regression modeling, be able to add orders of magnitude to Planck's Constant *h*, currently reported in (Newell and Tiesinga, 2019) to be 6.62607015×10^{-34} [J×s].

CONCLUSION

This paper demonstrates how **(*L*%+*E*%)** probability levels (Langford, 2021a) correlate with the work of Galileo, Newton, Einstein, Planck, and de Broglie (Langford, 2021b); which, together with temperature data estimated for immersion liquids and immersed-fragment interiors (Thermodynamics), show how applications of Quantum Mechanical Theory mesh seamlessly with Real-World RI data. At least some of the gap, that has previously made Quantum Mechanics seem to be so very strange when compared to Classical Physics, has been bridged.

ACKNOWLEDGEMENT

Comprehensive acknowledgments are provided at https://tinyurl.com/qt20n48o.

REFERENCES

Langford, SA. 2021[a]. Refractive index, a key to better petrography and to fundamental laws of Nature; *m*, *E*, and *W* Vacuum-Structure rest-mass calculations. Canadian Journal of Pure and Applied Sciences. 15(1):5133-5140.

Langford, SA. 2021[b]. A Portion of Vacuum-Structure Mass, Energy, and Weight. Canadian Journal of Pure and Applied Sciences. 15(1):5169-5178.

McCrone, WC., Draftz, RG. and Delley, JG. 1968. The Particle Analyst. Ann Arbor Science Publishers, Ann Arbor. pp. 224.

Newell, DB. and Tiesinga, E. 2019. NIST Special Publication 330, The International System of Units (SI). Eds. Newell, DB. and Tiesinga, E. NIST National Institute of Standards and Technology, U.S. Department of Commerce. pp. 138. DOI: https://doi.org/10.6028/NIST.SP.330-2019.

Received: Feb 9, 2021; Accepted: April 21, 2021